University of Saskatchewan
Subatomic Physics Internal Report

SPIR 140

# Calibration of the 5-paddle Flux Monitor

Rob Pywell

November 30, 2008, revised January 6, 2009

**Abstract**

The results of the analysis of the calibration of the 5-paddle flux monitor for the September/October 2008 blowfish runs at HIGS are presented. The flux monitor has met its design specifications of being able to determine the number of photons incident on it to within 2%.

## Contents

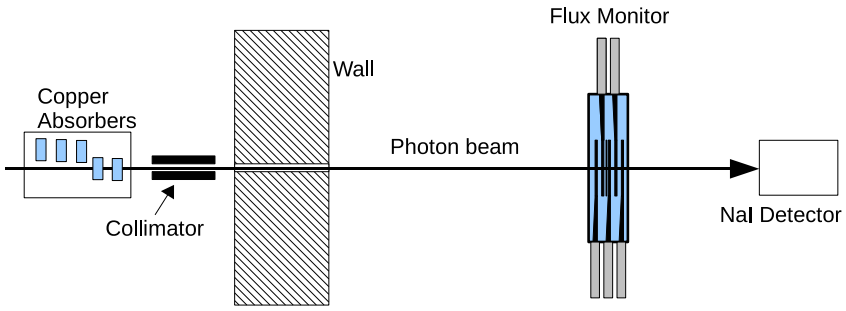


Figure 1: A schematic of the experimental arrangement used to characterize the photon flux monitor (not to scale).

# 1 Introduction

This document describes the calibration of the 5-paddle flux monitor as used in the September and October run period at HIGS during 2008. During this period measurements of photo-neutrons were performed using $D_2O$, $H_2O$ and Empty targets, Deuterated and undeuterated active targets, and $^6Li$, $^7Li$ and Empty targets. The photo-neutrons were detected using "Blowfish." The 5-paddle photon flux monitor was placed after the target (and Blowfish) and before a large NaI detector that could be moved into the beam for flux monitor calibration runs.

# 2 Calibration Runs

Many runs to determine the calibration of the monitor were performed at each of the 4 photon energies employed during the September-October 2008 running period. For each calibration run, a NaI detector was moved into the beam downstream of the flux monitor, and the target, normally in the centre of blowfish, was removed. In addition, the photon beam intensity was reduced by inserting copper absorbers into the beam line before the primary collimator so that the NaI would be able to count individual photons. A schematic of the experimental arrangement is shown in figure 1. The flux monitor calibration runs are summarized in table 1.

The table is presented in chronological order. In the table column 1 is the photon beam energy and column 2 is the lucid data acquisition run number. Column 3 is the rate in the flux monitor scaler during the live time which is listed in column 4. The total count in the flux monitor scaler during the live time is listed in column 6. Column 5 is the integral of the NaI spectrum which is, of course, recorded during the live time. An example of a NaI spectrum is shown in Figure 2 with the lower integration limit indicated by the vertical line. The integration omits the low energy background visible in the spectrum.

Table 1: Flux Monitor (FM) Calibration Runs

| Beam Energy (MeV) | Run | FM Rate (Hz) | Live Time (s) | NaI Sum | FM Count |
|---|---|---|---|---|---|
| 25 | 595 | 6.8 | 31.975 | 10031 | 217 |
| 25 | 663 | 6.7 | 434.5 | 150231 | 2932 |
| 25 | 664 | 72 | 775.03 | $3.115\times10^6$ | 55790 |
| 20 | 708 | 8.6 | 454.02 | 198150 | 3922 |
| 20 | 709 | 91 | 609.08 | $3.080\times10^6$ | 55533 |
| 35 | 857 | 19 | 362.89 | 378609 | 6827 |
| 35 | 858 | 265 | 22.24 | 324808 | 5889 |
| 20 | 891 | 11 | 365.73 | 203670 | 4151 |
| 20 | 892 | 75 | 156.48 | 645964 | 11715 |
| 25 | 921 | 6.3 | 1610.40 | 519540 | 10078 |
| 25 | 922 | 69 | 284.33 | $1.086\times10^6$ | 19550 |
| 30 | 951 | 7.2 | 126.496 | 42982 | 908 |
| 30 | 952 | 55 | 213.24 | 642477 | 11660 |
| 35 | 973 | 65 | 222.608 | 791070 | 14437 |

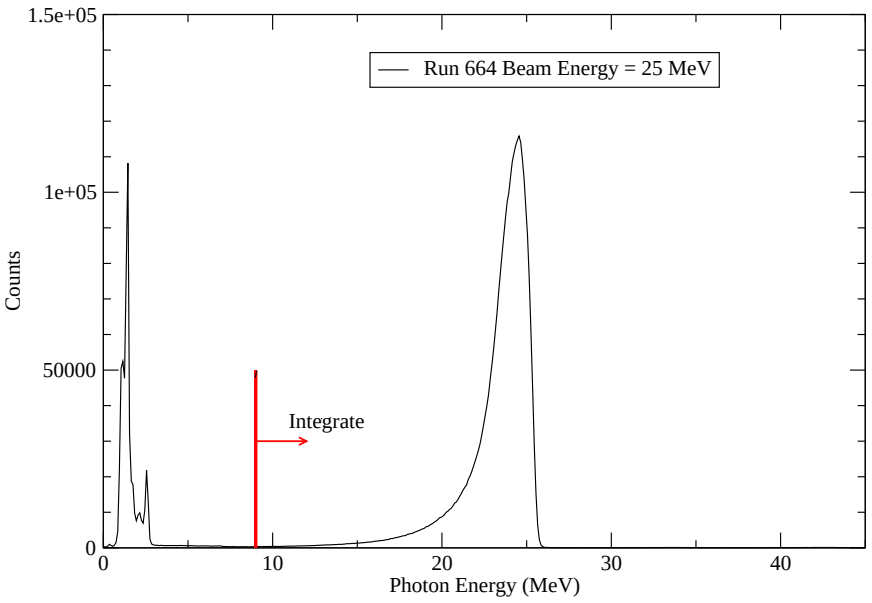


Figure 2: An example NaI spectrum for run number 664 at a beam energy of 25 MeV. The spectrum was integrated from 9 MeV up.

# 3 Calibration Analysis

If we define, for the live time of the measurement,

$N_\gamma$ = Number of gamma rays incident on the monitor,
$N_m$ = Number of measured gamma rays, i.e. the flux monitor counts,
$N_{NaI}$ = Number of gamma rays measured by the NaI detector, i.e. the NaI sum,

then we can define,

$\epsilon_m = N_m/N_\gamma$ = The Flux Monitor efficiency,
$f_m = 1/\epsilon_m$ = The Flux Monitor calibration factor.

To begin with we calculate,

$f'_m$ = The measured flux monitor calibration factor,

using

$$f'_m = \frac{(N_{NaI} - B_{NaI}T_{live})}{(N_m - B_m T_{live})} \tag{1}$$

where

$T_{live}$ = is the live time of the measurement,
$B_{NaI}$ = is the background rate in the integration region of the NaI spectrum (which was essentially zero for all runs), and
$B_m$ = is the background count rate of the flux monitor.

$B_m$ was difficult to determine accurately. Because of the triple coincidence requirement in the flux monitor the major contribution to the background is cosmic rays incident at angles such that it passed through the three paddles while missing the veto paddle. In addition there is a contribution from the room background resulting in a random coincidences producing a count. Several measurements were made to estimate the background count rate. These measurements were necessarily made while the beam was off. It was found that different results were obtained depending on how long the beam had been off before the measurement was made. Therefore, the best estimate of the background rate was determined from run 709 which was a 1 hour run taken just after the beam was turned off. This rate was $B_m = 0.70 \pm 0.02$ Hz. It must be assumed that this is approximately the rate when the beam is on and the beam intensity is reduced with the absorbers.

The measured calibration factor calculated using equation 1 and the above background rate for the runs listed in table 1 are plotted in figure 3 as a function of flux monitor count rate. It can be seen that the results are consistent within the errors of the measurements. (It is expected that the factor will vary slowly with energy.) It was found that the calibration factors determined for the low rate measurements varied dramatically with the background rate used. It was found that the background rate quoted above from run 709 gave results that were at least consistent with the calibration factors measured at higher flux monitor count rates. Nevertheless, in the subsequent analysis, only the measurements taken at flux monitor rates greater than 25 Hz were used. At these rates a factor of two uncertainty in $B_m$ resulted in a less than 0.5% change in the measured flux monitor calibration factor for most measurements.

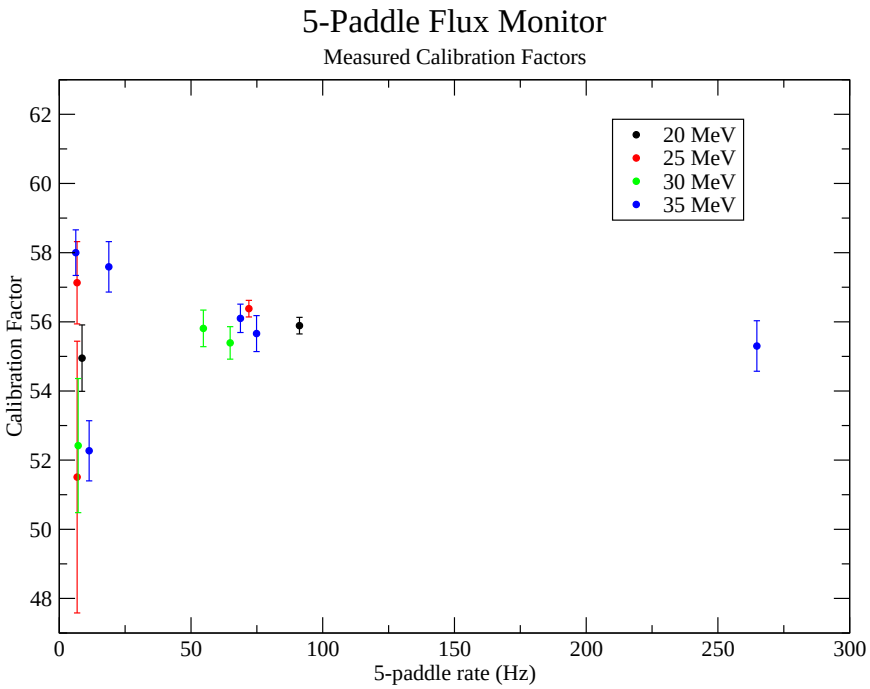


Figure 3: The measured calibration factor as a function of rate in the 5-paddle flux monitor for the 4 energies.

# 4 GEANT4 Simulation

A GEANT4[1] simulation of the experimental arrangement including the flux monitor and the NaI detector has been developed. The simulation includes all dimensions and materials in the flux monitor and the NaI detector and the relative positions of these two detectors and the primary collimator. The simulation assumes a uniform distribution of photons over the collimator opening. The simulation includes all relevant electromagnetic and hadronic interactions at these energies. From the simulation the spectrum from the flux monitor paddles and the NaI detector can be compared to the measured values.

During each experimental run a sample of the flux monitor spectra are recorded. An 'or' of all 5 discriminator outputs for the 5 paddles is used to generate a gate for an ADC connected to each paddle signal. A coincidence register also records which paddles were above its discriminator threshold.

The simulation is able to very well reproduce the spectra observed in the measurement. This can be seen in figure 4. The figure shows the spectra from the 5 paddles of the flux monitor when a beam of energy 25 MeV passes through it. The paddles are labeled 0 to 4 with paddle 0 at the upstream end and the aluminum absorber is between paddles 1 and 2. A count from the monitor is determined by a triple coincidence between paddles 2, 3 and 4 in anti-coincidence with the veto, paddle 1. In the figure the spectra for paddle 2, 3 and 4 are for the normal condition for a count i.e. in anti-coincidence with paddle 1. The spectra for paddles 0 and 1 are for the condition of a triple coincidence between paddles 0, 1 and 2,

which is used to determine the gain of the veto, paddle 1.

The energy calibration for each paddle was found by matching the single minimum ionizing peak (the lowest energy peak in each spectrum) to the energy determined from the simulation. The simulated spectrum was scaled by normalizing the integral in the energy range from 0.5 MeV to 1.5 MeV to the integral of the measured spectrum. The energy resolution of the paddles was adjusted in the simulation to match the measured spectra. It can be seen that the shapes of the measured spectra are well reproduced by the simulation. The dashed blue lines in the figure shows the discriminator thresholds for each paddle. The discriminator thresholds were determined from spectra incremented for a particular paddle with no coincidence requirement with other paddles but with the coincidence register bit set to indicate that it was above threshold.

A copy of the GEANT4 flux monitor simulation application is available at
`http://nucleus.usask.ca/ftp/pub/rob/flux-1.0.tgz`
The application works with Geant4.8.1.p01. A version that will work with latter releases of Geant4 will be forthcoming. The application requires the packages "LightOutput" available at
`http://nucleus.usask.ca/ftp/pub/rob/LightOutput-1.0.tgz`.
If output in Lucid[2] format is desired the package "G4Lucid" available at
`http://nucleus.usask.ca/~ward/G4Lucid/index.html`
will also be needed. (The G4Lucid package also requires Lucid to be installed on your system.)

# 5 Absorption Correction

The measured calibration factor $f'_m$ is not equal to the true calibration factor $f_m$ because not all gamma rays incident on the flux monitor reach, and are detected by, the NaI detector. The correction factor, defined by

$$c_{abs} = N_\gamma / N_{NaI}. \tag{2}$$

is determined from the simulation for each energy.

The true calibration factor is then given by

$$f_m = c_{abs} f'_m \tag{3}$$

The weighted mean of all measurements with flux monitor rates above 25 Hz was used to find the final true calibration factor. The results are summarized in table 2.

The true calibration factor can also be calculated from the simulation provided all parameters of the flux monitor are known to sufficient precision. The most critical parameter in this calculation is the thickness of the aluminum absorber. The efficiency of the flux monitor is almost directly proportional to this thickness. Unfortunately this thickness is not known to sufficient precision. Micrometer measurements of aluminum absorber thickness vary between 2.217 mm and 2.230 mm. The thickness of the absorber in the simulation was varied until the average efficiency for the four energies agreed with the measured average efficiency. This was achieved with an absorber thickness of 2.297 mm which was within the range of the measurements. With this absorber thickness the average measured calibration

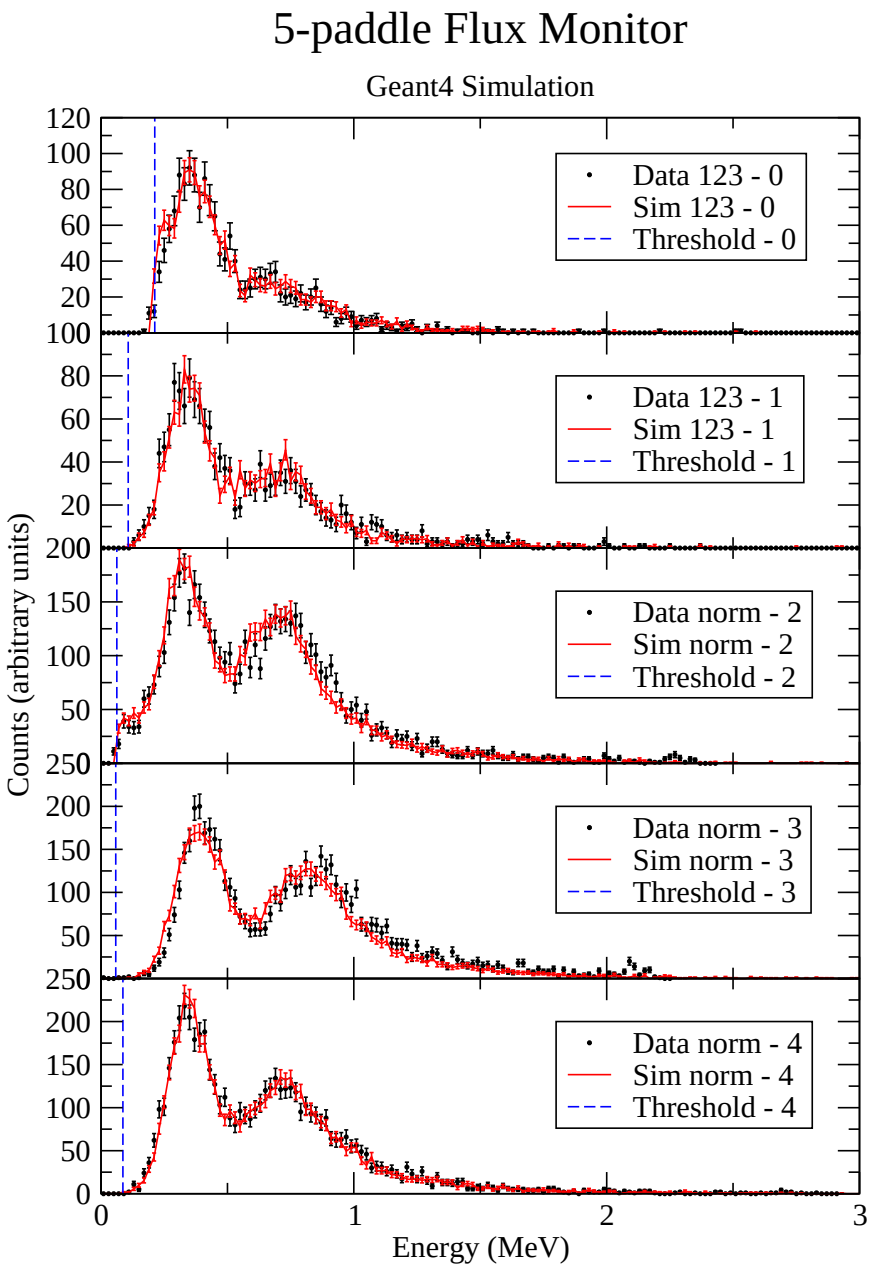


Figure 4: Spectra from the 5 paddles in the flux monitor compared to the simulation for a beam energy of 25 MeV.

Table 2: Measured flux monitor calibration factors after correction by the absorption factor.

| Beam Energy (MeV) | Absorption Factor $c_{abs}$ | Calibration Factor $f_m$ |
|---|---|---|
| 20 | 1.0504 ± 0.0001 | 58.68 ± 0.50 |
| 25 | 1.0405 ± 0.0001 | 58.63 ± 0.50 |
| 30 | 1.0338 ± 0.0001 | 57.33 ± 0.51 |
| 35 | 1.0291 ± 0.0001 | 58.02 ± 0.43 |

Table 3: Recommended Flux Monitor Calibration Factors

| Beam Energy (MeV) | Calibration Factor $f_m$ | Efficiency $\epsilon_m$ (%) |
|---|---|---|
| 20 | 59.01 ± 0.46 | 1.694 ± 0.013 |
| 25 | 58.52 ± 0.46 | 1.709 ± 0.013 |
| 30 | 58.03 ± 0.45 | 1.723 ± 0.013 |
| 35 | 57.54 ± 0.45 | 1.738 ± 0.013 |

factor for the four energies is 58.18 ± 0.35 while the average calibration factor from the simulation is 58.27 ± 0.22. These agree to within less than 0.5%. The absorption correction factors quoted in table 2 are calculated using this absorber thickness.

The measured and calculated calibration factors are plotted as a function of energy in figure 5.

The systematics as a function of energy displayed by the simulation are expected to be closer to the truth. Therefore the recommended calibration factors are as listed in table 3. There errors in table 3 reflect the uncertainty in normalizing the simulation to the measurement by varying the absorber thickness.

# 6 Rate Correction

The HIGS beam is not a 100% duty factor photon beam. The photon beam comes in bunches at a rate of 5.58 MHz or about 180 ns apart. The dead-time of the flux monitor is of the order 60 ns (about the width of the veto generated by the veto paddle). Therefore photons arriving in separate bunches will always be counted by the scaler if they are detected by the flux monitor. However more than one photon being detected in the flux monitor in a single bunch will be counted as only one. In fact this bunch rate limitation on the count rate of the flux monitor saves it from severe pileup effect at high photon rates.

The above calibration factors are measured at very low photon fluxes so that the probability of more than one photon being detected in a single bunch is extremely small. Therefore the measured efficiency, and the efficiency predicted by the GEANT4 simulation where one photon at a time is simulated, is an absolute efficiency appropriate only at low rates. At

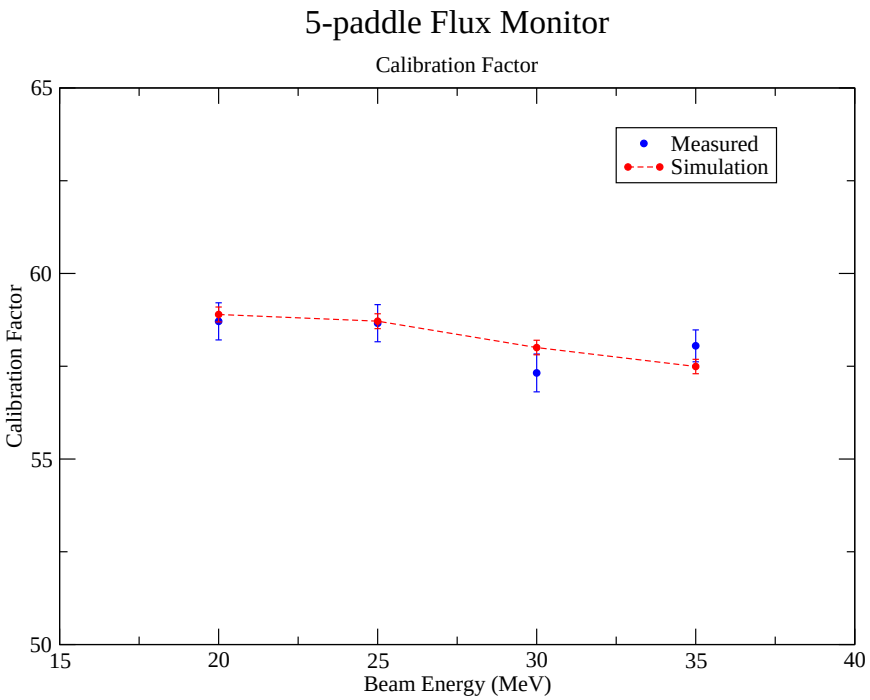


Figure 5: Measured calibration factors and calculated calibration factors for the 5-paddle flux monitor as a function of energy.

high photon rates a correction for multiple hits in a bunch must be made.

The number of photons detected is reduced when two or more photons are detected in a single bunch and are counted as only one. A further reduction occurs when a photon is detected, but another photon in the same bunch causes a hit in the veto paddle, thus killing the detected photon.

Therefore in order to calculate the correction at high rates the probability that a photon hitting the flux monitor will cause a hit in the veto (paddle 1) is needed. This information can be obtained from the simulation. The result for the four energies under consideration are listed in table 4.

A full calculation of the probability of getting a count from the flux monitor in a single

Table 4: Veto paddle hit efficiencies

| Beam Energy (MeV) | Efficiency $\epsilon_v$ (%) |
|---|---|
| 20 | $1.032 \pm 0.005$ |
| 25 | $1.043 \pm 0.005$ |
| 30 | $1.048 \pm 0.005$ |
| 35 | $1.066 \pm 0.005$ |

bunch is complicated and involves many terms. Such an expression is difficult to invert to calculate the number of gamma rays from the number of flux monitor counts. Fortunately a good approximation can found using the following simple argument.

We define,

$N_h = \epsilon_m N_\gamma$ = Number of hits on the flux monitor that have the potential to be counted.

So then,

$\mu_h = N_h/B$ = Average number of hits per bunch.

From Poisson statistics,

$$P_h(x_h, \mu_h) = \frac{{\mu_h}^{x_h}}{x_h!} e^{-\mu_h} \tag{4}$$

is the probability of $x_h$ hits in a bunch. Since one or more hits will be counted as one, the probability of a count will be,

$$P_h(x_h \geq 1, \mu_h) = 1 - P_h(0, \mu_h) = 1 - e^{-\mu_h} \tag{5}$$

But this hit may be vetoed if another photon in the bunch causes a hit in the veto paddle. The probability that this occurs may be estimated as follows. Defining

$\mu = N_\gamma/B =$ average number of photons in a bunch,

then

$\mu - \mu_h =$ average number of photons in a bunch that did not cause a detectable hit.

If

$\epsilon_v =$ veto efficiency = the probability that a photon causes a hit in the veto paddle,

then,

$\mu_v = (\mu - \mu_h)\epsilon_v =$ the average number of those photons that cause a hit in the veto paddle.

Therefore, from Poisson statistics, the probability that there is no hit in the veto paddle from these photons is

$$P_v(0, \mu_v) = e^{-\mu_v} \tag{6}$$

Therefore the total number of counts from the flux monitor is

$$\begin{aligned} N_m &= B P_v(0, \mu_v) P_h(x_h \geq 1, \mu_h) \\ &= B e^{-\epsilon_v(1-\epsilon_m)\frac{N_\gamma}{B}} (1 - e^{-\epsilon_m \frac{N_\gamma}{B}}) \end{aligned} \tag{7}$$

This expression must be inverted to calculate $N_\gamma$ from $N_m$. This is not easily done algebraically and so must be done numerically. A first order expansion of equation 7 that can be inverted algebraically does not provide sufficient accuracy for photon rates over about $8 \times 10^6$ Hz.

The correctness of equation 7 for calculating $N_\gamma$ was tested using three Monte-Carlo simulations. In the first simulation the number of counts in the flux monitor was determined bunch by bunch. For a given photon rate, the average number of photons hitting the monitor in a bunch was calculated. For each bunch Poisson statistics was used to select a number of photons. The true efficiency of the monitor was used to randomly determine how many of these photons caused a hit. Then the veto efficiency was used to randomly determine how many of the remaining photons caused a veto which removed the hit. After a suitable number of bunches the total number of photons hitting the monitor and the total number of counts from the monitor will be known.

In the second simulation the number of photons was again selected using Poisson statistics. Then, for each photon, the actual output from a GEANT4 simulation of the flux monitor (that fired one photon at a time) was used to determine which paddles recorded hits for a given photon. An 'or' of all the hit patterns in a given bunch was examined to determine if there was a hit (i.e. no hit in the veto and a triple coincidence for paddles 2, 3 and 4). Both these simulations gave the same results.

A third simulation was run using GEANT4 where multiple photons were fired in each geant event. Once again the number of photons fired was selected using Poisson statistics for a given photon rate. If the number of photons was zero the event was still recorded as a bunch.

In an actual experiment, both the total number of bunches $B$ and the total number of flux monitor hits $N_m$ during the live time of a measurement are recorded in scalers. Then using the known values of the efficiencies $\epsilon_m$ and $\epsilon_v$ the number of photons $N_\gamma$ can be calculated from equation 7. This was tested, using the first simulation, for a wide range of photon rates and the results are shown figure 6. The figure shows the error in the calculated number of photons if the rate correction was ignored (i.e. the number of photons was calculated by simply using $N_\gamma = N_m/\epsilon_m$.) After applying the rate correction it can be seen that equation 7 gives the correct number of photons to within 1%.

Also shown on figure 6 is one data point from the third simulation using the full GEANT4 simulation with multiple photons in each bunch. It can be seen that for this simulation too the correction using equation 7 gives excellent results.

The error in $N_\gamma$ depends on the uncertainties in $N_m$, $\epsilon_m$ and $\epsilon_v$ in the usual way.

$$(\delta N_\gamma)^2 = \left(\frac{\partial N_\gamma}{\partial N_m}\right)^2 {\delta N_m}^2 + \left(\frac{\partial N_\gamma}{\partial \epsilon_m}\right)^2 {\delta \epsilon_m}^2 + \left(\frac{\partial N_\gamma}{\partial \epsilon_v}\right)^2 {\delta \epsilon_v}^2 \tag{8}$$

The coefficients in equation 8 can be estimated from a leading order approximation of equation 7. The results are,

$$\frac{\partial N_\gamma}{\partial N_m} = \frac{1}{\epsilon_m}, \quad \frac{\partial N_\gamma}{\partial \epsilon_m} = -\frac{N_m}{{\epsilon_m}^2}, \quad \text{and} \quad \frac{\partial N_\gamma}{\partial \epsilon_v} = \frac{(1-\epsilon_m){N_m}^2}{{\epsilon_m}^2 B}. \tag{9}$$

The derivation of these coefficients is outlined in Appendix A.

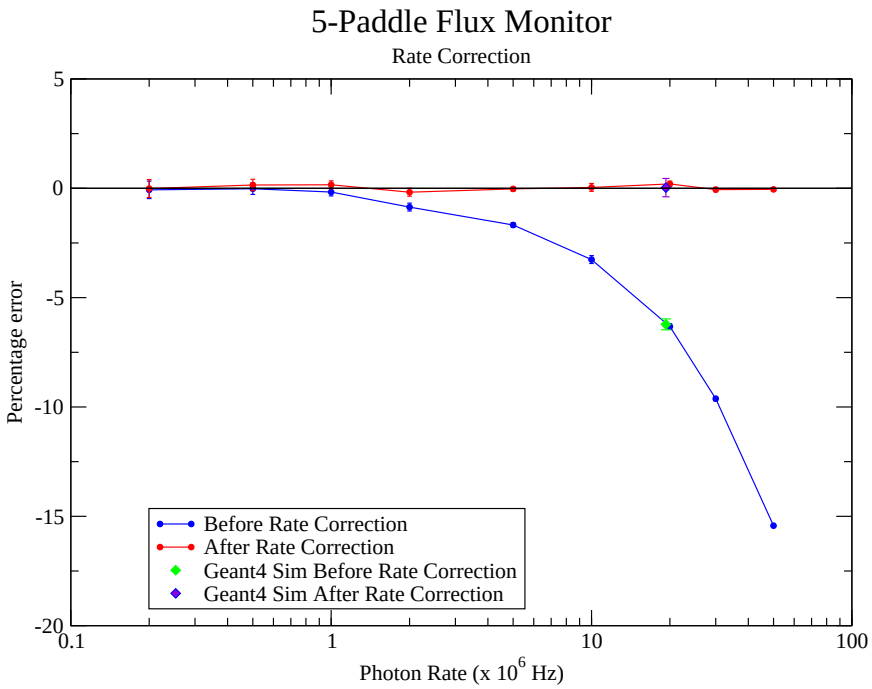


Figure 6: The percentage error in the number of photons as a function of photon rate. The errors without applying a rate correction and after applying a correction are shown.

In the calculation of the data points in figure 6 from the first simulation there was no error in the efficiencies $\epsilon_m$ and $\epsilon_v$ since these numbers were inputs to the simulation. Equation 7 does a surprisingly good job, given that it is not strictly a correct expression. A listing of the Perl code for the first simulation used for testing the rate correction, which includes a very simplistic algorithm for inverting equation 7, is given in Appendix B.

# 7 Other Rate Effects

Figure 7 shows the spectra from the flux monitor paddles at different rates. The spectra at a beam energy of 25 MeV taken at a very low photon rate is compared to the spectra taken at a rate of about $9 \times 10^6$ Hz. The gain of the paddles does not appear to change much with rate. Since the efficiency is only weakly dependent on gain this will have little effect on the efficiency of the monitor. There seems to be a decrease in resolution for some paddles, especially visible at low pulse heights. This appears to be associated with the gating of the ADC. This is confirmed by effects observed in the pedestals for the ADC for those paddles. An additional confirmation that the effect is related to the ADC comes from the fact that there appears to be counts in the spectra below the pedestal level. This would not be possible if the change in the signal occurred before it reached the discriminator. Therefore we believe the flux monitor scaler counts are unaffected by these effects observed in the spectra.

An increase in the background singles rate in the veto paddle at high beam fluxes would potentially decrease the efficiency of the flux monitor. This would have to be room back-

ground from other sources than the photons passing through the monitor which are already taken into account. Additional room background is a possibility since, as we noted above, we did observe background rates to change as a function of time after the beam was turned off. We have no evidence that such a background is very large and the efficiency of a single paddle to background is small since the paddles are thin. However this effect is something that should be measured in the future by moving the flux monitor out of the beam. If the rate of such background is less that 10 MHz the effect on the efficiency of the monitor will be less than 0.5%.

# 8 Target Absorption

Finally, for completeness, we note that the number of gamma rays calculated above is the number hitting the flux monitor, not the number entering the target.

There are two ways to deal with this. One is to run the flux monitor GEANT4 simulation again with a target in place. Then the values of $\epsilon_m$ and $\epsilon_v$ derived from the simulation will include target absorption effects and the number of gamma rays derived using the above procedure will be the number entering the target.

The second way is to make a correction, at least to a first approximation, is to use the mass attenuation coefficient $\mu/\rho$ of the target for the gamma ray energy in question. The absorption coefficient is $\mu = (\mu/\rho)\rho$ where $\rho$ is the density of the target. If the target thickness is $t$ and the number of gamma rays entering the target is $N_{\gamma 1}$, the number of gamma rays leaving the target is

$$N_\gamma = N_{\gamma 1} e^{-\mu t} \tag{10}$$

When calculating the cross section for a reaction it is important to include absorption along the length of the target. This is best accounted for by using a simulation. A first approximation can be made using the following analysis.

The number of gamma rays passing through a part of the target which is a distance $x$ from the start of the target is

$$N_\gamma(x) = N_{\gamma 1} e^{-\mu x} \tag{11}$$

The number of nuclear reactions, with cross section $\sigma$, that occur in a piece of the target of thickness $\Delta x$ at a distance $x$ from the start of the target is

$$N_R(x) = N_\gamma(x) n \sigma \Delta x \tag{12}$$

where $n$ is the number density of reaction centres in the target. The total number of reactions that occur in at target of thickness $t$ is then

$$N_R = \int_0^t N_\gamma(x) n \sigma dx \tag{13}$$

Using equation 11 we find

$$N_R = N_{\gamma 1} \frac{n\sigma}{\mu} \left(1 - e^{-\mu t}\right) \tag{14}$$

and then using equation 10

$$N_R = N_\gamma \frac{n\sigma}{\mu} \left(e^{\mu t} - 1\right) \tag{15}$$

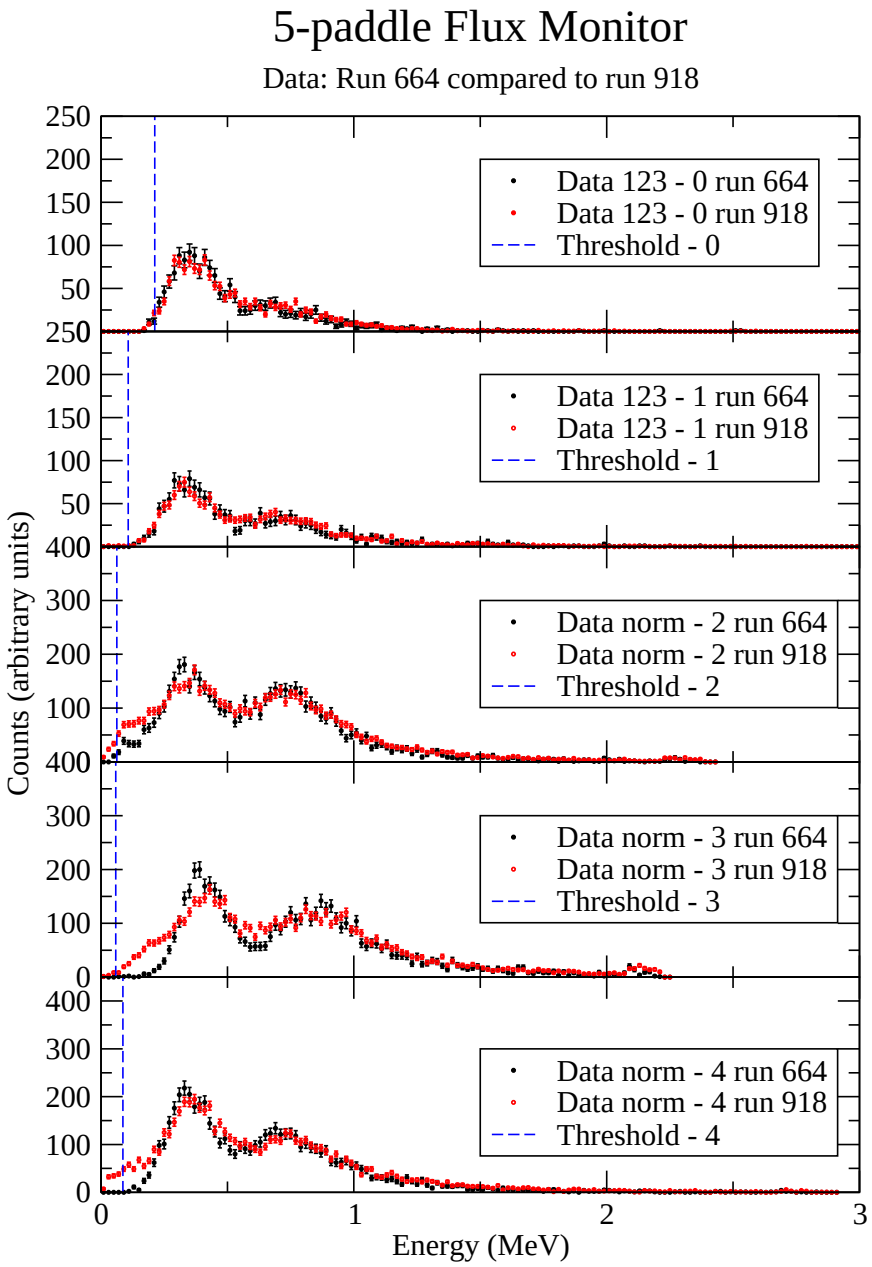


Figure 7: The spectra taken different photon rates. Run 664 is at a very low rate while run 918 is at a rate of about $9 \times 10^6$ Hz.

# 9 Conclusion

We have presented the results of measurements and calculations required to characterize the 5-paddle photon flux monitor. The monitor, after proper calibration, and after correction for rate effects, appears to meet its design goal of measuring the number of photons incident upon it during the live time of a measurement to within a systematic error of 2%. It has been shown that the efficiency of the monitor can be known to better that 1%. Therefore, with further work, and checks on the additional rate effects discussed in section 7, it may be possible to reduce the systematic error below 2% in the future.

# A Derivation of Error Coefficients

To second order, if $\epsilon_v N_\gamma/B$ and $\epsilon_m N_\gamma/B$ are small, equation 7 can be written

$$\frac{N_m}{B} = \left(1 - \epsilon_v(1-\epsilon_m)\frac{N_\gamma}{B}\right)\left(\epsilon_m \frac{N_\gamma}{B} - \frac{\epsilon_m^2 N_\gamma^2}{2B^2}\right).$$

In the form of a quadratic equation this is

$$\left(\frac{N_\gamma}{B}\right)^2 - \frac{1}{\epsilon_v(1-\epsilon_m)+\epsilon_m/2}\left(\frac{N_\gamma}{B}\right) + \frac{1}{\epsilon_m(\epsilon_v(1-\epsilon_m)+\epsilon_m/2)}\left(\frac{N_m}{B}\right) = 0,$$

or

$$\left(\frac{N_\gamma}{B}\right)^2 - \frac{1}{\epsilon'}\left(\frac{N_\gamma}{B}\right) + \frac{1}{\epsilon_m \epsilon'}\left(\frac{N_m}{B}\right) = 0$$

where $\epsilon' = \epsilon_v(1-\epsilon_m)+\epsilon_m/2$. The solution of this is

$$\frac{N_\gamma}{B} = \frac{1}{2}\left[\frac{1}{\epsilon'} \pm \sqrt{\frac{1}{\epsilon'^2} - \frac{4}{\epsilon_m \epsilon'}\frac{N_m}{B}}\right].$$

This can be written

$$\frac{N_\gamma}{B} = \frac{1}{2\epsilon'}\left[1 - \sqrt{1 - \frac{4\epsilon'}{\epsilon_m}\frac{N_m}{B}}\right],$$

where we have noted that the negative square root is the correct solution. We note that

$$\frac{4\epsilon'}{\epsilon_m}\frac{N_m}{B} \sim 4\epsilon'\frac{N_\gamma}{B} < 1$$

since $N_\gamma/B \sim 1-10$ and $\epsilon' \sim 0.02$. So we can use $(1-x)^{1/2} \approx 1 - 1/2x - 1/8x^2$ to show that

$$\frac{N_\gamma}{B} = \frac{1}{\epsilon_m}\frac{N_m}{B} + \frac{\epsilon'}{{\epsilon_m}^2}\left(\frac{N_m}{B}\right)^2.$$

So finally

$$N_\gamma = \frac{N_m}{\epsilon_m} + \frac{(\epsilon_v(1-\epsilon_m)+\epsilon_m/2)}{{\epsilon_m}^2}\frac{{N_m}^2}{B}.$$

The leading order term is as expected if there is no rate correction.

Taking the partial derivatives of this expression leads to the coefficients in equation 9. For the partial derivatives with respect to $N_m$ and $\epsilon_m$ we have used only the leading order term. This is good enough for an error estimate.

# B Rate Simulation Code

```
#!/usr/bin/perl

$gamma_rate = 10.0e6;
$bunch_rate = 5.58e6;
$true_efficiency = 0.01706;
$err_true_efficiency = 0.00006;
$veto_efficiency = 0.01041;
$err_veto_efficiency = 0.00005;

$ave_gamma_per_bunch = $gamma_rate / $bunch_rate;
printf "Average gammas per bunch = %.2f\n", $ave_gamma_per_bunch;

$n_bunch = 10000000;

$pois_prob_gamma[0] = exp(-$ave_gamma_per_bunch);
#print "prob[0] = $pois_prob_gamma[0]\n";
$n_pois_gamma = int(6*$ave_gamma_per_bunch);
if($n_pois_gamma < 3){$n_pois_gamma = 3;};
for($i = 1; $i <= $n_pois_gamma; $i++)
      {
      $pois_prob_gamma[$i] = $pois_prob_gamma[$i-1]
                  * $ave_gamma_per_bunch / $i;
      #print "prob[$i] = $pois_prob_gamma[$i]\n";
      }


$sum_gammas = 0;
for($i = 0; $i < $n_bunch; $i++)
      {
      # use poisson statistics to get the number of gammas
      # in this bunch
      $n_gamma = poisson_gamma();
      $sum_gammas += $n_gamma;
      #print "$i : $n_gamma\n";

      # find out how many of these caused a normal hit
      # that would be counted
      $n_hit = 0;
      for($j = 0; $j < $n_gamma; $j++)
            {
            if( rand() < $true_efficiency )
                  {
```

```
                $n_hit++;
                }
        }
    if($n_hit > 0)
        {
        # now look at the others and
        # decide if any of them caused a veto
        # (we already know that $n_hit photons
        # did not cause a veto)
        $vetoed = 0;
        for($j = $n_hit; $j < $n_gamma; $j++)
                {
                if( rand() < $veto_efficiency )
                        {
                        $vetoed = 1;
                        last;
                        }
                }
        if($vetoed == 0)
                {
                $num_detected++;
                }
        }
    }
printf "Gamma rate = %.1fe06\n", $gamma_rate/1000000.;
print "Number of bunches = $n_bunch\n";
print "Number of gammas = $sum_gammas\n";
print "Number of counts = $num_detected\n";
$exp_gammas = $num_detected/$true_efficiency;
$d_exp_gammas = sqrt($num_detected)/$true_efficiency;
printf "Non rate corrected number of gammas = %.0f +/- %.0f\n",
    $exp_gammas, $d_exp_gammas;
$fractional_error = ($exp_gammas - $sum_gammas) / $sum_gammas;
$d_fractional_error = $d_exp_gammas / $sum_gammas;
printf "Percentage error = %0.2f +/- %0.2f\n",
    $fractional_error*100., $d_fractional_error*100.;
#for($i = 0; $i <= $n_pois_gamma; $i++)
#    {
#     print "dist[$i] = $dist[$i]\n";
#     }
print "\n";

# naive correction ignoring vetos
$est_gammas = -$n_bunch / $true_efficiency
```

```
            * log(1.0 - $num_detected/$n_bunch);
printf "Naive (ignoring vetos) corrected number of gammas = %.0f\n",
            $est_gammas;

# now see if we can calculate the correct number of gammas

# first guess
$est_gammas = $num_detected / $true_efficiency;
$step_size = 0.05 * $est_gammas;
$dir = +1.0;

$diff1 = $num_detected - cal_count();
$est_gammas += $step_size * $dir;
$diff2 = $num_detected - cal_count();
      #print "diff1 = $diff1, diff2 = $diff2\n";
      #print "step_size = $step_size, dir = $dir\n";

$iter = 0;
while(abs($diff2)/$num_detected > 0.0001)
      {
      #print "est_gammas = $est_gammas\n";
      #print "diff1 = $diff1, diff2 = $diff2\n";
      #print "step_size = $step_size, dir = $dir\n";
      if($diff1*$diff2 < 0.)
            {
            # sign changed
            # so go the other direction in smaller steps
            $step_size /= 3.;
            $dir = -$dir;
            }
      else
            {
            if(abs(diff2) > abs(diff1) )
                  {
                  #wrong direction
                  $dir = -$dir;
                  }
            }

      $est_gammas += $step_size * $dir;
      $diff1 = $diff2;
      $diff2 = $num_detected - cal_count();
      }
```

```
#printf "Converged: Calculated Number of Gammas = %.0f\n",$est_gammas;

# estimate the error in number of gammas
$a = 1./$true_efficiency;
$b = $num_detected/$true_efficiency**2;
$c = (1.-$true_efficiency)/4./$true_efficiency**2
      * $num_detected**2 / $n_bunch;
# In this simulation there is no error in the true efficiency
# or the veto efficiency since these are inputs to the calculation.
$b = 0; $c = 0;
$err_est_gammas = sqrt(
      ($a)**2 *$num_detected
      + ($b*$err_true_efficiency)**2
      + ($c*$err_veto_efficiency)**2
      );
printf "Calculated Number of gammas = %.0f +/- %.0f\n",
      $est_gammas, $err_est_gammas;

$fractional_error = ($est_gammas - $sum_gammas) / $sum_gammas;
$d_fractional_error = $err_est_gammas / $sum_gammas;
printf "Percentage error = %0.2f +/- %0.2f\n",
      $fractional_error*100., $d_fractional_error*100.;exit;

sub cal_count
      {
      # $est_gammas is the current estimate of the number of gammas
      $n_m = $n_bunch * exp(-$est_gammas
            * (1. - $true_efficiency) * $veto_efficiency / $n_bunch)
            * (1.0 - exp(-$est_gammas * $true_efficiency / $n_bunch) );
      #print "Calulated num_counts = $n_m\n";
      return $n_m;
      }

sub poisson_gamma
      {
      if (rand() > $pois_prob_gamma[0])
            {
            my $i;
            do {
                  $i = int(rand()*$n_pois_gamma + 1);
                  if ($i > $n_pois_gamma) {$i = $n_pois_gamma;}
               }
            while ( rand() > $pois_prob_gamma[$i] );
            return $i;
```

```
        }
else
        {
        return 0;
        }
}
```

# References


[1] GEANT4 Collaboration, *Nucl. Inst. and Meth. A* 503 (2003) 250.

[2] D. Murray, et al., *LUCID User's Guide*.
`http://nucleus.usask.ca/technical_reports/report_index.html`.